

Multiphoton detachment of electrons from negative ions

G. F. Gribakin* and M. Yu. Kuchiev†

School of Physics, University of New South Wales, Sydney 2052, Australia

(Received 5 December 1996)

A simple analytical solution for the problem of multiphoton detachment from negative ions by a linearly polarized laser field is found. It is valid in the wide range of intensities and frequencies of the field, from the perturbation theory to the tunneling regime, and is applicable to the excess-photon as well as near-threshold detachment. Practically, the formulas are valid when the number of photons is greater than one. They produce the total detachment rates, relative intensities of the excess-photon peaks, and photoelectron angular distributions for the hydrogen and halogen negative ions, in agreement with those obtained in other, more numerically involved calculations in both perturbative and nonperturbative regimes. Our approach explains the extreme sensitivity of the multiphoton detachment probability to the asymptotic behavior of the bound-state wave function. Rapid oscillations in the angular dependence of the n -photon detachment probability are shown to arise due to interference of the two classical trajectories, which lead to the same final state after the electron emerges at diametrically opposite sides of the atom when the field is close to maximal.

[S1050-2947(97)03205-8]

PACS number(s): 32.80.Rm, 32.80.Gc, 32.80.Wr

I. INTRODUCTION

In this paper we present an analytical solution to the problem of multiphoton detachment from a negative ion by a linearly polarized laser field. It gives very reliable quantitative results for a wide range of intensities and frequencies of the laser field, from the weak-field regime, where the process is described by the perturbation theory, to the strong fields, where it proceeds as tunneling. The theory is valid when the number of photons n is large, but usually gives good results as soon as $n \geq 2$. We use it to calculate and examine various characteristics of the problem: the total multiphoton detachment rate, the n -photon detachment cross sections, the spectrum of excess-photon detachment (EPD) photoelectrons (the analogue of above-threshold ionization in atoms), and the peculiar photoelectron angular distributions.

There are two important physical properties of the multiphoton detachment process.

(i) The frequency of the laser field is much lower than the electron binding energy

$$\omega \ll |E_0|, \quad (1)$$

where $E_0 = -\kappa^2/2$ is the energy of the bound state (atomic units are used throughout). This means that multiphoton detachment is an *adiabatic problem*. The external field varies slowly in comparison with the period of electron motion in the system. Therefore, the general adiabatic theory [1–3] is applicable. As long as the laser field is weaker than the atomic field, the detachment probability is exponentially small with respect to the adiabaticity parameter $|E_0|/\omega \sim n$.

(ii) The process of multiphoton detachment takes place when the electron is far away from the atomic particle (see Sec. II), at *large distances*,

$$r \sim R = \left(\frac{\gamma}{\omega \sqrt{1 + \gamma^2}} \right)^{1/2} \gg 1, \quad (2)$$

where $\gamma = \omega \kappa / F$ is the Keldysh parameter and F is the field strength. In the weak field regime $\gamma \gg 1$, Eq. (2) gives $R \approx 1/\sqrt{\omega} \sim \kappa^{-1} \sqrt{2n} \gg 1$, where $\kappa \sim 0.3$ for a typical negative ion binding $|E_0| \sim 1$ eV. In the strong field regime $\gamma < 1$, estimate (2) yields $R \approx \sqrt{\gamma/\omega} = \kappa^{-1} \sqrt{F_0/F} \gg 1$, where $F_0 \equiv \kappa^3$ is the typical atomic electric field and $F \ll F_0$.

The two features, (i) and (ii), greatly simplify the multiphoton detachment problem. Owing to (ii), the final state of the electron can be described by the Volkov wave function [4], which takes into account the external field and neglects the atomic field. Moreover, the Volkov wave function describes explicitly the variation of the electron energy in the laser field. This makes it very convenient for application of the general adiabatic theory, as suggested by (i).

Calculations based on the Volkov final-state wave function were first done by Keldysh [3]. Subsequently, the idea was developed by Perelomov, Popov, and Terent'ev [5] and later reconsidered by Faisal [6] and Reiss [7]. This approach is usually supposed to give a correct qualitative picture of multiphoton processes. In this paper we demonstrate that, in fact, it produces very accurate quantitative results for the multiphoton detachment from negative ions. We reexamine and extend the Keldysh theory, paying particular attention to the following points. First, we show that the EPD can be described accurately by the theory. Originally, the theory was developed for low-energy photoelectrons [3] with kinetic energies much smaller than the binding energy. The present approach is valid at any photoelectron energy. Second, the angular distribution of photoelectrons is examined in detail. We show that a nontrivial oscillatory pattern of the angular distribution is caused by the simple and interesting physics. The photoelectron's escape from the atomic particle is most probable when the field reaches its maximum. There are two such instants in every period of the laser field $T = 2\pi/\omega$, say, $t = 0$ and $t = T/2$. As a result, there are two

*Electronic address: gribakin@newt.phys.unsw.edu.au

†Electronic address: kuchiev@newt.phys.unsw.edu.au

classical trajectories which lead to the same final state of the photoelectron. Interference of the corresponding amplitudes gives rise to an oscillatory angular dependence of the detachment rate. There is a similar effect in the single-photon detachment in the presence of a static electric field, where the interference takes place between the two trajectories of the electron emitted up or down field [8,9].

Estimate (2) leads to a further simplification of the problem, since the initial bound-state wave function of the atomic system should also be considered at large distances, where it can be replaced by its simple asymptotic form. The complicated behavior of the wave function inside the atom and the corresponding many-electron dynamics have little influence on the multiphoton detachment. In contrast, use of the wave function with incorrect asymptotic behavior, e.g., that corresponding to the Hartree-Fock binding energy, introduces an error, which is exponentially large with respect to \sqrt{n} . Such sensitivity has been noticed in the perturbation theory calculations of the two- and three-photon detachment from H^- [10].

There have been a large number of papers where multiphoton detachment from the hydrogen and halogen negative ions is investigated. Perturbation theory calculations include those based on the Hartree-Fock approximation [11], adiabatic hyperspherical approach [10], model potential [12], a configuration-interaction procedure [13], and the Lippmann-Schwinger equation [14]. There are also numerous nonperturbative methods, such as the Floquet close-coupling method [15], complex-scaling generalized pseudospectral method [16], non-Hermitian Floquet Hamiltonian method [17], and the R -matrix Floquet theory [18,19]. All the above methods rely on much more involved numerical calculations than those needed in our analytical approach. However, we believe that the present theory provides accurate answers for most of the multiphoton detachment problems. For illustration purposes, we reproduce a variety of results obtained earlier, including the n -photon cross sections, total detachment probability, EPD spectrum and photoelectron angular distributions for a large range of frequencies and intensities of the field (Sec. III). We believe that in some cases our results are more accurate than those obtained previously, due to the correct asymptotic behavior of the bound-state wave function we use.

The good accuracy we have achieved within the Keldysh-type theory is quite useful for the multiphoton detachment problem. On the other hand, its validity is very important for the development of an adiabatic theory of more complicated phenomena, such as double ionization [20–22].

The formulas obtained in this paper can be used to estimate probabilities of multiphoton ionization of neutral atoms. However, the influence of the Coulomb field of the positive ion on the wave function of the photoelectron cannot be neglected [23,24] and our results for the multiphoton ionization would be less reliable.

II. THEORY

A. Basic equations

Consider the removal of a valence electron from an atom or a negative ion by the laser field $\mathbf{F}(t) = \mathbf{F}\cos\omega t$. The differ-

ential detachment rate can be written as the sum over n -photon processes [see Appendix A, Eq. (A8)]

$$dw_n = 2\pi \sum_n |A_{pn}|^2 \delta(E_p - E_0 - n\omega) \frac{d^3p}{(2\pi)^3}, \quad (3)$$

where A_{pn} is the amplitude of the n -photon process

$$A_{pn} = \frac{1}{T} \int_0^T \Psi_p^*(\mathbf{r}, t) V_F(t) \Psi_0(\mathbf{r}, t) d\mathbf{r} dt, \quad (4)$$

$\Psi_0(\mathbf{r}, t) = e^{-iE_0 t} \Phi_0(\mathbf{r})$ is the wave function of the initial electron state in the atomic potential $U(\mathbf{r})$

$$\left[\frac{p^2}{2} + U(\mathbf{r}) \right] \Phi_0(\mathbf{r}) = E_0 \Phi_0(\mathbf{r}), \quad (5)$$

$V_F(t)$ is the interaction with the laser field,

$$V_F(t) = -e\mathbf{r} \cdot \mathbf{F}(t), \quad (6)$$

in the length gauge, $e = -1$ for the electron, and $\Psi_p(\mathbf{r}, t)$ is the continuous spectrum solution of the time-dependent Schrödinger equation with the quasienergy $E_p = \mathbf{p}^2/2 + F^2 e^2/4\omega^2$. It describes the outgoing photoelectron in the laser field with the translational momentum \mathbf{p} , and $F^2 e^2/4\omega^2$ is the electron quiver energy due to the field. The subscript n in A_{pn} reminds one that the amplitude must be calculated at $E_p = E_0 + n\omega$, provided by the energy conservation in Eq. (3).

As we show below, the detachment probability is determined by the asymptotic behavior of the bound-state wave function at large distances. This means that the role of electron correlations in the multiphoton detachment of a single electron is small, provided $\Phi_0(\mathbf{r})$ correctly represents the asymptotic behavior of the true many-electron wave function of the system

$$\Psi_N(\mathbf{r}_1, \dots, \mathbf{r}_{N-1}, \mathbf{r}) \underset{r \gg 1}{\simeq} \Psi_{N-1}(\mathbf{r}_1, \dots, \mathbf{r}_{N-1}) \Phi_0(\mathbf{r}), \quad (7)$$

where Ψ_N is the ground-state wave function of the N -electron system, and Ψ_{N-1} is the wave function of the $N-1$ -electron atomic residue.

If we neglect the influence of the atomic potential $U(\mathbf{r})$ on the photoelectron, the final state is given by the Volkov wave function

$$\Psi_p(\mathbf{r}, t) = \exp \left[i(\mathbf{p} + \mathbf{k}_t) \cdot \mathbf{r} - \frac{i}{2} \int^t (\mathbf{p} + \mathbf{k}_{t'})^2 dt' \right], \quad (8)$$

where $\mathbf{k}_t = e \int^t \mathbf{F}(t') dt'$ is the classical electron momentum due to the field. By omitting the lower integration limit we mean that we set its contribution to zero, as if the integration is performed from $-\infty$ and the integrand is switched on adiabatically. For the Volkov function (8) this gives the same phase as in [21], $-(i/2) \int_0^t (\mathbf{p} + \mathbf{k}_{t'})^2 dt' + i\mathbf{p}\mathbf{F}/\omega^2$, and provides $\Psi_p(\mathbf{r}, t)$ with a convenient symmetry property with respect to inversion:

$$\Psi_{-p}(\mathbf{r}, t) = \Psi_p(-\mathbf{r}, t + T/2) \exp(iE_p T/2). \quad (9)$$

The wave function (8) satisfies the Schrödinger equation

$$i\frac{\partial\Psi_{\mathbf{p}}}{\partial t}=\left[\frac{p^2}{2}+V_F(t)\right]\Psi_{\mathbf{p}}. \quad (10)$$

The neglect of the short-range potential $U(\mathbf{r})$ for the photoelectron is justified in multiphoton processes, e.g., in the multiphoton detachment from negative ions (see end of Sec. II B).

Using the complex conjugates of Eqs. (8) and (10) and $i\partial\Psi_0/\partial t=E_0\Psi_0$, we transform amplitude (4) into

$$A_{\mathbf{p}n}=\frac{1}{T}\int_0^T\left[E_0-\frac{(\mathbf{p}+\mathbf{k}_t)^2}{2}\right]\tilde{\Phi}_0(\mathbf{p}+\mathbf{k}_t) \times \exp\left[\frac{i}{2}\int_0^t(\mathbf{p}+\mathbf{k}_{t'})^2 dt'-iE_0 t\right] dt, \quad (11)$$

where $\tilde{\Phi}_0(\mathbf{q})$ is the Fourier transform of $\Phi_0(\mathbf{r})$

$$\tilde{\Phi}_0(\mathbf{q})=\int d\mathbf{r}e^{-i\mathbf{q}\cdot\mathbf{r}}\Phi_0(\mathbf{r}). \quad (12)$$

Note that in the velocity gauge

$$V_F(t)=-\frac{e}{c}\mathbf{A}(t)\cdot\mathbf{p}+\frac{e^2}{2c^2}\mathbf{A}^2(t), \quad \mathbf{A}(t)=-c\int_0^t\mathbf{F}(t')dt', \quad (13)$$

the Volkov wave function looks simpler,

$$\Psi_{\mathbf{p}}(\mathbf{r},t)=\exp\left[i\mathbf{p}\cdot\mathbf{r}-\frac{i}{2}\int_0^t(\mathbf{p}+\mathbf{k}_{t'})^2 dt'\right]. \quad (14)$$

This gauge, which apparently ‘‘leads to an analytical simplicity’’ [7],

$$A_{\mathbf{p}n}=\frac{1}{T}\left(E_0-\frac{\mathbf{p}^2}{2}\right)\tilde{\Phi}_0(\mathbf{p})\int_0^T \times \exp\left[\frac{i}{2}\int_0^t(\mathbf{p}+\mathbf{k}_{t'})^2 dt'-iE_0 t\right] dt, \quad (15)$$

is less physical though than the length gauge in this problem. The amplitude (4) is not gauge invariant when $U(\mathbf{r})$ is neglected for the final state [compare (11) with (15)], except for the zero-range s -wave initial state $\Phi_0(\mathbf{r})=Ar^{-1}e^{-\kappa r}/\sqrt{4\pi}$. The length gauge interaction (6) emphasizes large distances, where the bound-state wave function $\Phi_0(\mathbf{r})$ has a well-defined asymptotic behavior. We will see in the next section that this gives it a major advantage over the velocity gauge. In the limit $\omega\rightarrow 0$ the length-gauge calculation reproduces the static-field result [25,26].

B. Adiabatic approximation

For multiphoton processes the integral over time in the amplitude (11) contains a rapidly oscillating exponent $\exp[iS(\omega t)]$, where $S(\omega t)\sim 2\pi n$ is the coordinate-independent part of the classical action

$$S(\omega t)=\frac{1}{2}\int_0^t(\mathbf{p}+\mathbf{k}_{t'})^2 dt'-E_0 t. \quad (16)$$

This makes the amplitude $A_{\mathbf{p}n}$ exponentially small and the integral $\int_0^T\dots dt$ should be calculated using the saddle-point method. The positions of the saddle points are given by $dS(\omega t)/dt=0$, which yields

$$(\mathbf{p}+\mathbf{k}_t)^2+\kappa^2=0. \quad (17)$$

The saddle-point method in this problem has simple and important physical contents. The two terms on the right-hand side of Eq. (16) describe the energy of the electron in the initial and final states, E_0 and $(\mathbf{p}+\mathbf{k}_t)^2/2$, respectively. According to the general adiabatic theory [2], the transition from the initial to the final state happens at the moment in time when their energies are equal. This is exactly the meaning of Eq. (17).

Note that condition (17) coincides with the positions of singularities of the Fourier transform $\tilde{\Phi}_0(\mathbf{p}+\mathbf{k}_t)$ in the amplitude (11). Indeed, the general asymptotic form of $\Phi_0(\mathbf{r})$ is

$$\Phi_0(\mathbf{r})\underset{r\gg 1}{\simeq}Ar^{\nu-1}\exp(-\kappa r)Y_{lm}(\hat{\mathbf{r}}), \quad (18)$$

where $\nu=Z/\kappa$, Z is the charge of the atomic residue ($\nu=Z=0$ for the negative ion), and $\hat{\mathbf{r}}=\mathbf{r}/r$ is the unit vector. It is easy to see that due to (18) the Fourier transform (12) is singular at $q^2=-\kappa^2$. Using [27] we derive the following asymptotic form of $\tilde{\Phi}_0(\mathbf{q})$ for $q\rightarrow\pm i\kappa$:

$$\tilde{\Phi}_0(\mathbf{q})=4\pi A(\pm)^l Y_{lm}(\hat{\mathbf{p}})\frac{(2\kappa)^\nu\Gamma(\nu+1)}{(q^2+\kappa^2)^{\nu+1}}, \quad (19)$$

where $(\pm)^l\equiv(\pm 1)^l$ corresponds to $q\rightarrow\pm i\kappa$.

Therefore, when the length-form amplitude is calculated by the saddle-point method, we do not need to know the behavior of the bound-state wave function in the whole space. In contrast, when using the velocity-form amplitude (15), the value of the Fourier transform for the true final-state momentum \mathbf{p} is needed. To calculate it one must know the exact wave function at all distances, including $r\sim 1$. What makes the problem even harder is that many-electron correlations become essential there.

Equation (17) for the saddle points, presented explicitly as

$$\left(\mathbf{p}+\frac{e\mathbf{F}}{\omega}\sin\omega t_\mu\right)^2+\kappa^2=0, \quad (20)$$

defines complex values t_μ where the transition from the bound state into the Volkov state takes place. Equation (20) has two pairs of complex conjugate roots in the interval $0\leq\text{Re}(\omega t)<2\pi$. According to the general theory of adiabatic transitions [2], in the case where the final-state energy $E_{\mathbf{p}}$ is greater than the initial energy E_0 , we should take into account the two saddle points in the upper half-plane of complex t .

Changing the integration variable to ωt and substituting the asymptotic expression for the Fourier transform near the singularity (19), we can write amplitude (11) as the sum over the two saddle points

$$\begin{aligned}
& -\frac{1}{2\pi} \sum_{\mu=1,2} \int [(\mathbf{p}+\mathbf{k}_t)^2 + \kappa^2] \\
& \times \frac{4\pi A(\pm)^l Y_{lm}(\hat{\mathbf{p}}_\mu)(2\kappa)^\nu \Gamma(\nu+1)}{2[(\mathbf{p}+\mathbf{k}_t)^2 + \kappa^2]^{\nu+1}} \exp[iS(\omega t)] d(\omega t), \quad (21)
\end{aligned}$$

where the integral is taken over the vicinity of the μ th saddle point, $\hat{\mathbf{p}}_\mu$ is the unit vector in the direction of $\mathbf{p}+(e\mathbf{F}/\omega)\sin\omega t_\mu$, and the two signs in (\pm) correspond to $\mu=1,2$. Note that for the initial electron state bound by short-range forces, as in a negative ion, the integrand in (21) has no singularity ($\nu=0$) and the application of standard saddle-point formulas is straightforward. Having the general case in mind, we will calculate the amplitude for arbitrary ν , taking into account the singularity at the saddle point. This is also useful if one wants to calculate the amplitude in the original form (4) without using the transformation that leads to Eq. (11).

Using $dS(\omega t)/d(\omega t)=[(\mathbf{p}+\mathbf{k}_t)^2 + \kappa^2]/2\omega$, we can rewrite Eq. (21) as

$$\begin{aligned}
& -2\pi A\Gamma(\nu+1) \left(\frac{\kappa}{\omega}\right)^\nu \frac{1}{2\pi} \sum_{\mu=1,2} (\pm)^l Y_{lm}(\hat{\mathbf{p}}_\mu) \\
& \times \int \frac{\exp[iS(\phi)]}{[S'(\phi)]^\nu} d\phi, \quad (22)
\end{aligned}$$

where $\phi=\omega t$. In the vicinity of the saddle point ϕ_μ , $S'(\phi_\mu)=0$, we have $S'(\phi)\simeq S''(\phi_\mu)(\phi-\phi_\mu)$. The contribution of this saddle point is then given by the following integral:

$$\int \frac{\exp[iS(\phi)]}{[S'(\phi)]^\nu} d(\phi) = \frac{1}{[S''(\phi_\mu)]^\nu} \int \frac{\exp[iS(\phi)]}{(\phi-\phi_\mu)^\nu} d\phi, \quad (23)$$

which is calculated in Appendix B.

The explicit form of the action (16) is

$$S(\phi) = n\phi - \xi \cos\phi - \frac{z}{2} \sin 2\phi, \quad (24)$$

where $z=e^2F^2/4\omega^3$ is the mean quiver energy of the electron in the laser field in units of ω , $\xi=e\mathbf{F}\mathbf{p}/\omega^2$ depends on the angle θ between the photoelectron momentum \mathbf{p} and the field \mathbf{F} , and we put $E_p-E_0=n\omega$ due to the energy conservation in (3). Thus, we obtain the final expression for the amplitude by the saddle-point method:

$$\begin{aligned}
A_{\mathbf{p}n} & = -2\pi A\Gamma(1+\nu/2)2^{\nu/2} \left(\frac{\kappa}{\omega}\right)^\nu \sum_{\mu=1,2} (\pm)^l Y_{lm}(\hat{\mathbf{p}}_\mu) \\
& \times \frac{(c_\mu + is_\mu)^n \exp[-ic_\mu(\xi + zs_\mu)]}{\sqrt{2\pi(-iS''_\mu)^{\nu+1}}}, \quad (25)
\end{aligned}$$

where

$$\sin\omega t_\mu = (-\xi \pm i\sqrt{8z(n-z)-\xi^2})/4z \equiv s_\mu, \quad (26)$$

$$\cos\omega t_\mu = \pm\sqrt{1-s_\mu^2} \equiv c_\mu, \quad (27)$$

$$S''_\mu = c_\mu(\xi + 4zs_\mu), \quad (28)$$

and the signs \pm correspond to the two saddle points $\mu=1,2$. The usual definition of the spherical harmonics [28]

$$\begin{aligned}
Y_{lm}(\vartheta, \varphi) & = \frac{1}{\sqrt{2\pi}} e^{im\varphi} (-1)^{\frac{m+|m|}{2}} \left[\frac{2l+1}{2} \frac{(l-|m|)!}{(l+|m|)!} \right]^{1/2} \\
& \times P_l^{|m|}(\cos\vartheta), \quad (29)
\end{aligned}$$

is generalized naturally to calculate $Y_{lm}(\hat{\mathbf{p}}_\mu)$ for complex vectors by setting

$$\cos\vartheta = \frac{(\mathbf{p}+\mathbf{k}_t) \cdot \mathbf{F}}{\sqrt{(\mathbf{p}+\mathbf{k}_t)^2 F}} = \left(1 + \frac{p_\perp^2}{\kappa^2}\right)^{1/2}, \quad (30)$$

where the last equality is valid at the saddle points, and $p_\perp = p\sin\theta$ is the component of \mathbf{p} perpendicular to \mathbf{F} . The real physical angle θ should not be confused with the complex angle ϑ from Eqs. (29) and (30). The azimuthal angle φ is the same in both cases.

Using (9) and the symmetry of the spherical harmonics Y_{lm} , one can show that the amplitude (4) has the following symmetry properties: $A_{\mathbf{p}n} \rightarrow (-1)^{n+l} A_{\mathbf{p}n}$, upon inversion $\mathbf{p} \rightarrow -\mathbf{p}$ ($\theta \rightarrow \pi - \theta$, $\varphi \rightarrow \varphi + \pi$), and $A_{\mathbf{p}n} \rightarrow (-1)^{n+l+m} A_{\mathbf{p}n}$, upon reflection in the plane perpendicular to the direction of the field ($\theta \rightarrow \pi - \theta$). Consequently, the amplitude is zero for \mathbf{p} perpendicular to the field, if $n+l+m$ is odd.

It is easier to look at the physics behind Eqs. (25)–(28) in the case where the photoelectron momentum is small, $p \ll \kappa$. The following simpler formulas for the saddle points can be obtained from (26)–(28) by setting $\xi=0$:

$$\sin\omega t_\mu = \pm i\gamma, \quad \cos\omega t_\mu = \pm\sqrt{1+\gamma^2}, \quad S''_\mu = i\gamma\sqrt{1+\gamma^2}\frac{F^2}{\omega^3}, \quad (31)$$

where $\gamma=\kappa\omega/F$ is the Keldysh parameter. Thus, for small photoelectron momenta the saddle points are $\omega t_1 = i\sinh^{-1}\gamma$ and $\omega t_2 = \pi + i\sinh^{-1}\gamma$, and the detachment takes place at the two instances when the external field is maximal, $t=0$ and $T/2$ on the real axis. Accordingly, the total amplitude (25) is the sum of the two contributions from these points. This results in oscillations in the photoelectron angular distribution, which we discuss in greater detail below.

The original approach used in [3,5] was to expand Eqs. (26) and (27) and the action (24) in powers of p/κ to the second order (see Sec. IID2), thus obtaining corrections to (31). In this regime, γ remains the main parameter which determines the probability of multiphoton detachment [29]. However, the applicability of the saddle-point result (25) is essentially narrowed by such expansion (Sec. III).

The adiabatic nature of the problem allows us to estimate the radial distances that are important in the multiphoton detachment process. We have already seen that the saddle points in the integral in (11) coincide with the poles of the Fourier transform $\tilde{\Phi}_0(\mathbf{q})$. The form of $\tilde{\Phi}_0(\mathbf{q})$ at $q \rightarrow \pm i\kappa$ is given by the behavior of $\Phi_0(\mathbf{r})$ at $r \rightarrow \infty$. To estimate the

essential distances look at Eq. (22). The range of ϕ where the integral is saturated is determined by $|S''(\phi_\mu)(\delta\phi)^2| \sim 1$, which gives $\delta\phi \sim |S''(\phi_\mu)|^{-1/2}$. The corresponding range of momenta $\mathbf{p} + \mathbf{k}$, is given by

$$\delta q \sim \frac{F}{\omega} \cos\phi_\mu \delta\phi \sim \left(\frac{\omega \sqrt{1 + \gamma^2}}{\gamma} \right)^{1/2} \equiv \frac{1}{R}, \quad (32)$$

where we use Eq. (31). The essential distances are obtained from $r\delta q \sim 1$, which yields estimate (2). It is important that $R \gg 1$ in both weak- and strong-field regimes. This makes the Keldysh approach valid for short-range potentials. There is another physical reason which helps to clarify why the atomic potential can be neglected for the photoelectron. When a large number of photons is absorbed by the photoelectron, higher-angular-momentum partial waves are populated. The influence of the short-range potential upon them is small. For a given electron momentum p the important l values can be estimated as $l \sim pR$. In the perturbation theory regime this estimate yields $l \sim (p/\kappa)\sqrt{n}$, which suggests that the spread of the probability of finding the photoelectron with given l is described by a random walk of n steps.

Estimate (2) also explains the extreme sensitivity of the multiphoton detachment rates to the asymptotic behavior of the bound-state wave function. Suppose a bound-state wave function characterized by κ' instead of the true κ is used. The error in the amplitude (4) introduced by replacing κ by κ' comes in as a factor $\exp[-\Delta\kappa R]$, where $\Delta\kappa = \kappa' - \kappa$. The value of R is large; thus, even a small $\Delta\kappa$ can produce an exponential error in the amplitude. Using the perturbation-theory regime estimate of R we obtain the error factor of $\exp[-2(\Delta\kappa/\kappa)\sqrt{2n}]$ for the detachment rate.

C. Detachment rates

The differential n -photon detachment rate for the electron in the initial state lm is obtained from Eqs. (3) and (25) after integration over φ and p ,

$$\begin{aligned} \frac{dw_n}{d\Omega} &= \frac{pA^2}{4\pi} \left(\frac{\kappa}{\omega} \right)^{2\nu} 2^\nu \Gamma^2(1 + \nu/2)(2l+1) \frac{(l-|m|)!}{(l+|m|)!} \\ &\times |P_l^{|m|}(\sqrt{1+p^2\sin^2\theta/\kappa^2})|^2 \\ &\times \left| \sum_{\mu=1,2} (\pm)^{l+m} \frac{(c_\mu + is_\mu)^n}{\sqrt{2\pi(-iS''_\mu)^{\nu+1}}} \exp[-ic_\mu(\xi \right. \\ &\left. + zs_\mu) \right]^2, \end{aligned} \quad (33)$$

where $p = \sqrt{2(n\omega - F^2/4\omega^2 + E_0)}$ is the photoelectron momentum determined by the energy conservation and $\nu=0$ for negative ions. According to the symmetry properties of A_{pn} , the differential n -photon detachment rate is exactly zero at $\theta = \pi/2$ for odd $n+l+m$.

The total n -photon detachment rate of the lm state is obtained by integrating (33),

$$w_n^{(lm)} = 2\pi \int_0^\pi \frac{dw_n}{d\Omega} \sin\theta d\theta, \quad (34)$$

and if we are interested in the total detachment rate for a closed shell, the sum over m and the electron spin projections must be completed:

$$w_n = 2 \sum_{m=-l}^l w_n^{(lm)}. \quad (35)$$

The dominant contribution to this sum is given by the $m=0$ state, since it is extended along the direction of the field (see Sec. IID2).

It is very easy to take the effect of fine-structure splitting into account. The two fine-structure components $j=l \pm \frac{1}{2}$ of a closed shell are characterized by different binding energies $|E_0|$ and values of κ . The n -photon detachment rate for the j sublevel is then given by

$$\frac{dw_n^{(j)}}{d\Omega} = \frac{2j+1}{2l+1} \sum_{m=-l}^l \frac{dw_n}{d\Omega}, \quad (36)$$

which is exactly what one would expect from naive statistical considerations.

Of course, one can easily obtain the total detachment rate by summing the n -photon rates over n . The smallest n is given by the integer part of $[(|E_0| + F^2/4\omega^2)/\omega] + 1$.

D. Limits

There are two limits which can be usefully explored with the help of Eq. (33). The first is the perturbation theory limit, where the detachment rate is proportional to the n th power of the photon flux $J = cF^2/(8\pi\omega)$, and the process is described by the generalized n -photon cross section

$$\frac{d\sigma_n}{d\Omega} = \frac{dw_n}{d\Omega} J^{-n}. \quad (37)$$

The other is the low-photoelectron energy limit studied earlier in [3,5]. It enables one to recover the static-field results [25,26].

1. Perturbation-theory limit

To obtain the perturbation-theory limit, it is convenient to rewrite the saddle-point equation (26) for $\sin\omega t_\mu$ in the following form:

$$s_\mu = \frac{\omega}{F} (p_\parallel \pm i\sqrt{\kappa^2 + p_\perp^2}), \quad (38)$$

where $p_\parallel = p\cos\theta$ is the momentum component parallel to the field. The weak-field regime $\gamma \gg 1$ infers $|s_\mu| \gg 1$, hence we obtain for $\cos\omega t_\mu$

$$c_\mu = \pm \sqrt{1 - s_\mu^2} \simeq -is_\mu + \frac{i}{2s_\mu} + O(s_\mu^{-2}). \quad (39)$$

Using Eqs. (38) and (39) to calculate the amplitude (25) for $\nu=0$, and retaining only the leading term in c_μ everywhere, except in $c_\mu + is_\mu$, where the second term is necessary, we arrive at the following n -photon detachment cross section:

$$\begin{aligned} \frac{d\sigma_n}{d\Omega} &= \frac{pA^2\omega}{4\pi^2\sqrt{2n\omega}}(2l+1)\frac{(l-|m|)!}{(l+|m|)!} \\ &\times |P_l^{|m|}(\sqrt{1+p_\perp^2/\kappa^2})|^2 \left(\frac{\pi e}{nc\omega^2}\right)^n \\ &\times \frac{\exp(p_\parallel^2/\omega)}{\sqrt{\kappa^2+p_\perp^2}} [1+(-1)^{n+l+m}\cos\Xi], \quad (40) \end{aligned}$$

where $p = \sqrt{2n\omega - \kappa^2}$, $c \approx 137$ is the speed of light, $e = 2.71 \dots$, and Ξ is the momentum-dependent contribution to the relative phase of the two saddle-point terms in the amplitude,

$$\Xi = (2n+1)\tan^{-1}\frac{p_\parallel}{\sqrt{\kappa^2+p_\perp^2}} + \frac{p_\parallel\sqrt{\kappa^2+p_\perp^2}}{\omega}. \quad (41)$$

$$\begin{aligned} \frac{dw_n}{d\Omega} &= \frac{pA^2\omega\gamma}{2\pi|E_0|\sqrt{1+\gamma^2}} \frac{1}{(2^{|m|}|m|!)^2} \frac{2l+1}{4\pi} \frac{(l+|m|)!}{(l-|m|)!} \exp\left\{-2\frac{|E_0|}{\omega}\left[\left(1+\frac{1}{2\gamma^2}\right)\sinh^{-1}\gamma - \frac{\sqrt{1+\gamma^2}}{2\gamma}\right]\right\} \\ &\times \exp\left[-\left(\sinh^{-1}\gamma - \frac{\gamma}{\sqrt{1+\gamma^2}}\right)\frac{p^2}{\omega}\right] \exp\left(-\frac{\gamma p^2 \sin^2\theta}{\omega\sqrt{1+\gamma^2}}\right) \left(\frac{p\sin\theta}{\kappa}\right)^{2|m|} \left[1+(-1)^{n+l+m}\cos\left(\frac{2\kappa p\cos\theta\sqrt{1+\gamma^2}}{\omega\gamma}\right)\right]. \quad (42) \end{aligned}$$

This formula coincides with Eq. (53) of Ref. [5]. The $\cos(\dots)$ in the last square brackets of Eq. (42) appears due to the interference between the contributions of the two saddle points in amplitude (25) and is the analogue of $\cos\Xi$ in Eq. (40). It determines the oscillatory behavior of the angular dependence of the n -photon detachment rate, which would otherwise simply peak along the direction of the field $\theta=0$, or $\theta=\pi$, for $m=0$.

Formula (42) also shows clearly that the detachment rate for the states with $m \neq 0$ is much smaller than that of $m=0$, due to the factor $(p\sin\theta/\kappa)^{2|m|}$. It comes from the leading term in the expansion of the associated Legendre polynomial $P_l^{|m|}(x)$ in Eq. (33) at $x \approx 1$.

As shown by Perelomov, Popov, and Terent'ev [5], in the limit $\omega \rightarrow 0$ Eq. (42) allows one to recover the well-known formula for the ionization rate in the static electric field F [26]

$$\begin{aligned} w_{\text{stat}} &= \frac{A^2}{2\kappa^{2\nu-1}} \frac{(2l+1)(l+|m|)!}{2^{|m|}|m|!(l-|m|)!} \left(\frac{2F_0}{F}\right)^{2\nu-|m|-1} \\ &\times \exp\left(-\frac{2F_0}{3F}\right) \quad (43) \end{aligned}$$

for negative ion case $\nu=0$. It has been shown recently [30] that the account of the polarization potential $-\alpha e^2/2r^4$ acting between the outer electron and the atomic residue in the negative ion changes the numerical pre-exponential factor in Eq. (43). However, this correction is not very large, e.g., it

This phase varies with the ejection angle of the photoelectron from $\Xi_0 = (2n+1)\tan^{-1}(p/\kappa) + p\kappa/\omega$ to $-\Xi_0$, and can be quite large, even for the lowest n process, $p \sim \sqrt{\omega}$, $\Xi_0 \sim \sqrt{n}$, thus producing oscillations in the photoelectron angular distribution. Note that in accordance with the general symmetry properties, the cross section is zero at $\theta = \pi/2$, when $n+l+m$ is odd.

2. Low photoelectron energies and the static-field limit

Another simplification of the general formula (33) is achieved when the energy of the photoelectron is low compared to the binding energy $p^2 \ll \kappa^2$. Then, following [3,5] one can expand the action $S(\phi_\mu)$ and other quantities calculated at the saddle points up in powers of p to the second order. For $\nu=0$, which corresponds to the multiphoton detachment from a negative ion, we obtain

increases the detachment rate for Ca^- by a factor of 2, in spite of the large polarizability $\alpha(\text{Ca}) = 170$ a.u.

It is worth noting that the perturbation theory formula (40) and the low electron energy limit (42) have a common range of applicability. If we use $p \ll \kappa$ in the first and take the perturbation theory limit $\gamma \gg 1$ in the second, the two formulas yield identical results.

III. NUMERICAL RESULTS AND DISCUSSION

In this section we use the formulas we obtained within the adiabatic theory to calculate the photodetachment rates, EPD spectra, and photoelectron angular distributions for H^- and halogen negative ions. These are the most studied species so far, which enables us to make comparisons with results of other calculations. Our aim is to show that our theory achieves good accuracy in describing multiphoton detachment in both perturbative and strong-field regimes.

To apply the theory, all we need is the asymptotic parameters A and κ of the corresponding bound-state wave functions. The values of A are tabulated in various sources and we use those from [32]. The values of κ are calculated using the corresponding binding energies $\kappa = \sqrt{2|E_0|}$. They are taken from the electron affinity tables [33], or obtained by combining those with the fine-structure intervals of the atomic ground states [34], when we consider the detachment of $p_{1/2}$ electrons from the halogens.

In Fig. 1 we present the generalized n -photon detachment cross sections for H^- obtained by integrating the differential cross sections from Eq. (40) with $A = 0.75$ and $\kappa = 0.2354$

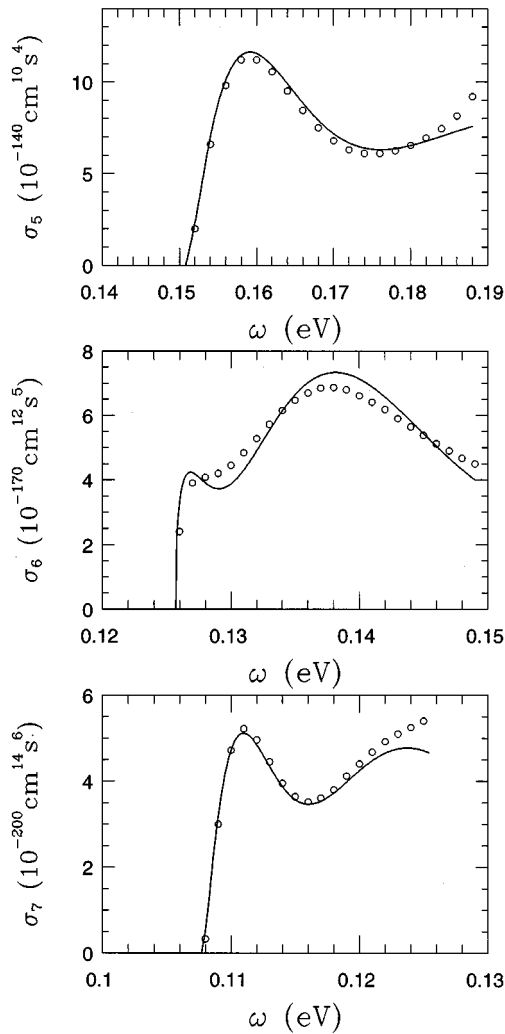


FIG. 1. Frequency dependence of the generalized n -photon detachment cross sections for H^- , $n=5,6,7$. Solid curve: present calculation, Eq. (40), integrated over angles; open circles: perturbation-theory calculations of Laughlin and Chu [12].

over θ . The cross section has been multiplied by 2 to account for the two spin states [cf. Eq. (36) with $l=0$, $j=1/2$]. The results of the perturbation-theory calculations [12] are shown for comparison. In the latter, the interaction of the electron with the atomic core was described by a model potential which accounted for the polarizational attraction between the electron and the atomic core, and was chosen to reproduce the binding energy of H^- , as well as the electron-hydrogen scattering phase shifts. Figure 1 shows that there is good agreement between our results and those of [12]. We checked that even for $n=3$ the difference does not exceed 20% at the cross section maximum.

Laughlin and Chu note [12] that their model-potential results are close to those obtained in [10] using the hyperspherical method, which accounts for correlations between the two electrons in H^- . They are also in agreement with the two-electron perturbation-theory calculations of [14] and the recent R -matrix Floquet-theory calculations [18], which also take into account electron correlations. The main idea behind those approaches was to reproduce the negative-ion wave function as correctly as possible at all distances, particularly

near the atomic core. This idea is favored by the experience gained from a number of problems, such as the single-photon detachment, electron-atom scattering, etc., where electron correlations are indeed very important. However, as shown above, the multiphoton problem under consideration proves to be different. Absorption of several quanta is dominated by large distances satisfying inequality (2). The complicated behavior of the wave function inside the atomic core turns out to be inessential. This is the main reason for the good agreement we observe in Fig. 1.

To check our theory in the nonperturbative regime, where one must use Eq. (33), the EPD spectra of H^- for the three large field intensities $I=10^{10}$, 5×10^{10} , and 10^{11} W/cm², of the 10.6- μ m radiation, $\omega=0.0043$ a.u., are presented in Table I. For these parameters, the electron quiver energy, or the ponderomotive energy shift, in units of ω , $z=F^2/4\omega^3=0.894$, 4.472, and 8.945, and the Keldysh parameter $\gamma=1.895$, 0.847, and 0.599, respectively. For given ω , absorption of a minimum of 7 photons is required. The ponderomotive threshold shift changes this number to $n_{\min}=8$, 11, and 16. The calculation of the detachment rates from Eqs. (33)–(36) has been done using *Mathematica* [31]. For the smallest intensity, the lowest EPD peak $n=8$ dominates the total detachment rate, whereas for the higher intensities many peaks in the EPD spectrum can be observed.

The detachment rates in Table I are compared with those obtained in the nonperturbative calculations of Telnov and Chu [17]. They describe their method as a complex-scaling generalized pseudospectral technique applied to the solution of the time-independent non-Hermitian Floquet Hamiltonian for the complex quasienergies and use the accurate model potential from [12] to describe the interaction of the electron with the atomic residue.

There is good overall agreement between the two calculations. The discrepancy usually does not exceed a few per cent, and is slightly larger for higher EPD peaks and smaller field intensities. The latter is somewhat puzzling, since there is good agreement in the perturbation-theory limit for the seven-photon cross section at $\omega=0.0043$ a.u.:

$$\sigma_7 = 3.537 \times 10^{-200} \text{ cm}^{14} \text{ s}^6 \text{ [Eq. (40) integrated over angles],}$$

$$\sigma_7 = 3.639 \times 10^{-200} \text{ cm}^{14} \text{ s}^6 \text{ (result of [17]).}$$

In Fig. 2 we show the angular dependence of the photoelectron peaks for $n=16, 17, 18$, and 19, at $I=10^{11}$ W/cm². We have checked that their shapes, as well as those for other n and intensities, are practically identical to the angular distributions presented in Figs. 5–7 of [17]. Also shown in Fig. 2 are the differential detachment rates obtained from Eq. (42). It works quite well for the two lowest n , but the agreement becomes poor with the increase of the photoelectron energy, e.g., for $n=19$, where $p/\kappa \approx 0.75$.

It is worth stressing again that the remarkable oscillatory behavior is caused by the interference of the two saddle-point contributions in Eq. (33), or, in other words, the interference between the electron waves emitted at the two instants separated by $T/2$, when the field reaches its maximum. The geometrical phase difference that determines the oscillations of $\cos(\dots)$ in Eq. (42) can be calculated classically. Suppose that the electron is considered free at the moment

TABLE I. The EPD spectra of H^- in the strong laser field of $\omega=0.0043$ a.u. The detachment rates calculated by our saddle-point method (SP), Eq. (33), $A=0.75$ and $\kappa=0.235$, are compared with the non-perturbative results by Telnov and Chu [17].

n	n -photon detachment rate (a.u.)					
	$I=10^{10}$ W/cm ²		$I=5\times 10^{10}$ W/cm ²		$I=10^{11}$ W/cm ²	
	SP	[17]	SP	[17]	SP	[17]
8	6.69×10^{-10}	7.12×10^{-10}				
9	1.92×10^{-10}	2.03×10^{-10}				
10	4.08×10^{-11}	4.32×10^{-11}				
11	4.99×10^{-12}	5.26×10^{-12}	5.44×10^{-7}	4.07×10^{-7}		
12	7.24×10^{-13}	7.86×10^{-13}	4.68×10^{-7}	4.88×10^{-7}		
13	2.03×10^{-13}	2.27×10^{-13}	3.57×10^{-7}	3.69×10^{-7}		
14			1.24×10^{-7}	1.30×10^{-7}		
15			9.54×10^{-8}	9.72×10^{-8}		
16			8.28×10^{-8}	8.52×10^{-8}	4.31×10^{-6}	4.32×10^{-6}
17			4.72×10^{-8}	4.88×10^{-8}	3.09×10^{-6}	3.14×10^{-6}
18			1.99×10^{-8}	2.06×10^{-8}	2.55×10^{-6}	2.48×10^{-6}
19			7.59×10^{-9}	7.87×10^{-9}	1.24×10^{-6}	1.24×10^{-6}
20			3.73×10^{-9}	3.94×10^{-9}	1.28×10^{-6}	1.22×10^{-6}
21			2.71×10^{-9}	2.92×10^{-9}	1.01×10^{-6}	1.01×10^{-6}
22			2.18×10^{-9}	2.37×10^{-9}	4.99×10^{-7}	5.05×10^{-7}
23			1.62×10^{-9}	1.77×10^{-9}	3.74×10^{-7}	3.64×10^{-7}
24			1.09×10^{-9}	1.18×10^{-9}	4.37×10^{-7}	4.25×10^{-7}
25			6.62×10^{-10}	7.17×10^{-10}	4.32×10^{-7}	4.28×10^{-7}
26			3.72×10^{-10}	4.02×10^{-10}	3.34×10^{-7}	3.34×10^{-7}
27			1.95×10^{-10}	2.10×10^{-10}	2.11×10^{-7}	2.12×10^{-7}
28			9.69×10^{-11}	1.04×10^{-10}	1.16×10^{-7}	1.17×10^{-7}
29					6.23×10^{-8}	6.26×10^{-8}
30					3.88×10^{-8}	3.94×10^{-8}
31					3.17×10^{-8}	3.26×10^{-8}
32					3.02×10^{-8}	3.14×10^{-8}
33					2.90×10^{-8}	3.03×10^{-8}
34					2.62×10^{-8}	2.75×10^{-8}
Sum	9.07×10^{-10}	9.66×10^{-10}	1.76×10^{-6}	1.67×10^{-6}	1.61×10^{-5}	1.61×10^{-5}

when it escapes the atomic particle. Its classical coordinate is then given by $\mathbf{r}(t) = \int^t \mathbf{k}_t dt' = (\mathbf{F}/\omega^2) \cos \omega t$. At the two instants t_μ when the adiabatic transition takes place, we have

$$\mathbf{r}(t_\mu) = \pm \frac{\mathbf{F}}{\omega^2} \sqrt{1 + \gamma^2} = \pm \frac{\mathbf{F}}{F} \frac{\kappa \sqrt{1 + \gamma^2}}{\gamma \omega},$$

where Eq. (31) is used for small momenta $p \ll \kappa$. Note that though t_μ are complex, the corresponding electron coordinates are real. These points located at the opposite sides of the atomic particle are sources of the two electron waves emitted at the angle θ with respect to \mathbf{F} . The geometrical phase is obtained by multiplying the base $|\mathbf{r}(t_1) - \mathbf{r}(t_2)|$ by the projection of the electron momentum on the direction of the field $p \cos \theta$.

Our results for halogen negative ions are presented in Fig. 3 and Table II. They have been obtained from Eqs. (40) and (36) for comparison with the perturbation-theory calculations [11] at the Nd:YAG laser frequency $\omega=0.0428$ a.u. In that work, the nonrelativistic Hartree-Fock wave functions of the valence np electrons were used, together with experimental threshold energies. The photoelectron was described in the plane-wave approximation. This approximation is equivalent

to our use of the Volkov wave function in the perturbation-theory limit. As shown in the earlier works by Crance [35], the multiphoton detachment results obtained in the plane-wave approximation are close to those obtained using the frozen core Hartree-Fock wave functions of the photoelectron.

The shapes of angular distributions presented in Fig. 3 are quite close to those in Fig. 2 of Ref. [11], although quantitative comparison is not feasible due to the use of an arbitrary vertical scale in [11].

The absolute values of the n -photon detachment cross sections from our calculations and [11] compare reasonably on a logarithmic scale for all cases shown in Table II. However, there is a systematic discrepancy. To find its origin let us recall that the multiphoton detachment rate is very sensitive to the asymptotic behavior of the bound-state wave function (see end of Sec. II B). In [11] the Hartree-Fock wave functions have been used. Their asymptotic behavior $\exp(-\kappa_{\text{HF}} r)$ is different from the correct $\exp(-\kappa r)$, based on the experimental value of κ . Thus, to account for the discrepancy in Table II, the Hartree-Fock-based results should be multiplied by the factor

$$\sim \exp[2(\kappa_{\text{HF}} - \kappa)R], \quad (44)$$

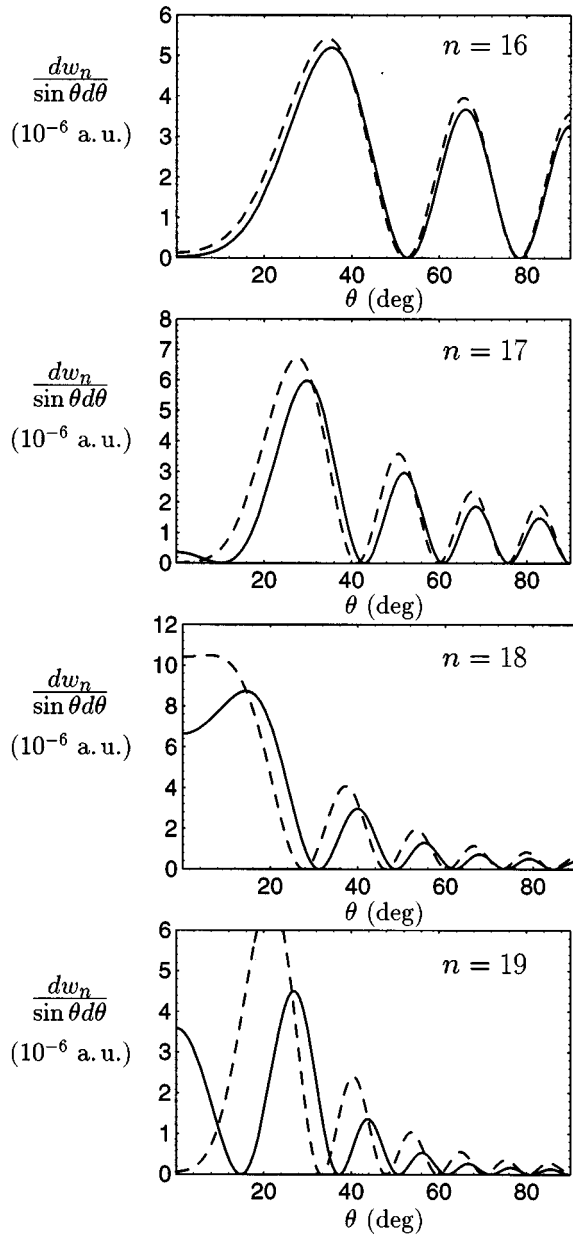


FIG. 2. Differential n -photon detachment rates of H^- in the strong laser field, $\omega=0.0043$ a.u., $I=10^{11}$ W/cm^2 , $z=8.945$, $\gamma=0.599$. Solid curve: “exact” saddle-point calculation, Eq. (33); dashed curve: low photoelectron energy limit, Eq. (42). Channels with $n < 16$ are closed.

where, according to (2), $R \approx 1/\sqrt{\omega}$. Formula (44) shows that when $\kappa_{\text{HF}} > \kappa$ the Hartree-Fock-based calculations underestimate the detachment rate, while for $\kappa_{\text{HF}} < \kappa$ they overestimate it.

The Hartree-Fock values of κ_{HF} are 0.602, 0.545, 0.528, and 0.508, for the outer np subshell of F^- , Cl^- , Br^- , and I^- , respectively. Examination of the lowest n cross sections throughout Table II shows that the qualitative explanation of the discrepancy based on (44) is correct. For example, for F^- where $\kappa_{\text{HF}}=0.6$ and $\kappa=0.5$, formula (44) gives 2.6, whereas the ratio of the three-photon detachment cross sections for F^- , $j=3/2$, in Table II is 4.3. Also, the best agree-

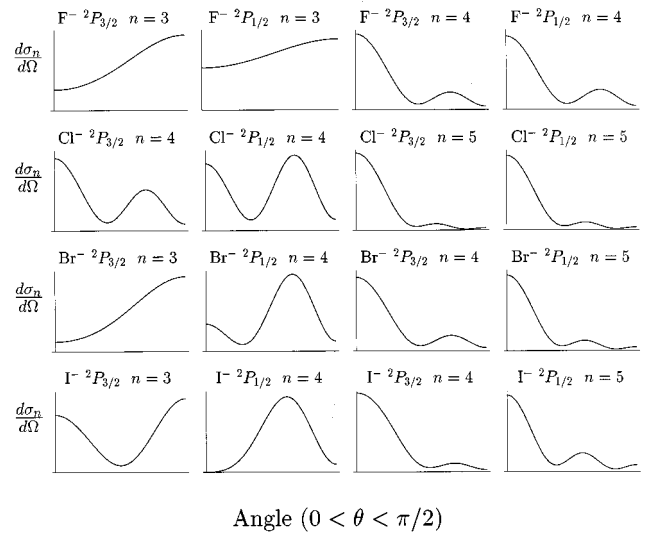


FIG. 3. Differential n -photon cross sections for the electron detachment from the halogen negative ions, which leaves the atom in the $^2P_{3/2}$ or $^2P_{1/2}$ states Eqs. (40) and (36).

ment in Table II is achieved for Br^- , $j=1/2$, where κ_{HF} is very close to the correct value. Therefore, we conclude that the incorrect asymptotic behavior of the Hartree-Fock wave functions can produce significant errors in the multiphoton detachment rates. This must be kept in mind when comparisons are made between different n -photon detachment calculations [19].

IV. SUMMARY

The main result of our work is that the adiabatic-theory approach to the multiphoton problems originally suggested by Keldysh is more powerful and accurate than is generally believed. It yields accurate multiphoton detachment rates for negative ions and reveals a number of interesting details about the physics of the problem: the role of large distances and asymptotic behavior of the bound-state wave function and the origin of oscillations in the angular distribution of photoelectrons. The formulas obtained in the paper allow one to make simple and reliable estimates of the n -photon detachment rates for $n \geq 2$ in both perturbative and nonperturbative regimes.

ACKNOWLEDGMENTS

We would like to thank V. V. Flambaum, W. R. Johnson, and O. P. Sushkov for useful discussions, and V. N. Ostrovsky for providing us with a reference. M. K. is thankful to L. Kuchieva for assistance with his earlier work on the subject. This work has been supported by the Australian Research Council.

APPENDIX A: CALCULATION OF TRANSITION RATES IN A STRONG PERIODIC FIELD

Suppose the system is in the initial state

$$\psi_0(t) = e^{-iE_0 t} \phi_0, \quad H_0 \phi_0 = E_0 \phi_0$$

of the time-independent Hamiltonian H_0 , and a periodic field $V(t) = V(t+T)$ is turned on adiabatically. We assume that

TABLE II. Comparison of the n -photon detachment cross sections from the halogen negative ions obtained by the saddle-point method (SP), Eqs. (40) and (36), with the perturbation-theory calculations by Crance [11] at $\omega = 0.0428$ a.u. For each n , $\log\sigma_n^{(j)}$ is shown, $\sigma_n^{(j)}$ being in units of $\text{cm}^2 \text{s}^{n-1}$; $j = 3/2$ and $1/2$ for the ${}^2P_{3/2}$ and ${}^2P_{1/2}$ final states of the atom.

Ion and its parameters	n	$\log\sigma_n^{(3/2)}$		n	$\log\sigma_n^{(1/2)}$	
		SP	[11]		SP	[11]
Fluorine	3	-81.62	-82.25	3	-82.01	-83.21
$A = 0.7$	4	-113.45	-114.06	4	-113.81	-114.39
$\kappa_{3/2} = 0.4998$	5	-145.36	-145.87	5	-145.71	-146.21
$\kappa_{1/2} = 0.5035$	6	-177.40	-177.75	6	-177.74	-178.08
Chlorine	4	-113.14	-113.42	4	-113.53	-113.74
$A = 1.3$	5	-145.05	-145.26	5	-145.47	-145.46
$\kappa_{3/2} = 0.5156$	6	-177.05	-177.12	6	-177.45	-177.49
$\kappa_{1/2} = 0.5233$	7	-209.14	-209.08	7	-209.53	-209.44
Bromine	3	-80.99	-81.23	4	-113.52	-113.52
$A = 1.4$	4	-112.81	-113.06	5	-145.51	-145.46
$\kappa_{3/2} = 0.4973$	5	-144.73	-144.85	6	-177.48	-177.31
$\kappa_{1/2} = 0.5300$	6	-176.77	-176.75	7	-209.55	-209.25
Iodine	3	-80.59	-80.85	4	-113.35	-113.10
$A = 1.8$	4	-112.27	-112.46	5	-145.48	-145.13
$\kappa_{3/2} = 0.4742$	5	-144.25	-144.31	6	-177.45	-176.98
$\kappa_{1/2} = 0.5423$	6	-176.33	-176.29	7	-209.50	-208.93

this field can be strong, so that the lowest-order perturbation theory is inapplicable. The time-dependent wave function of the system

$$i\frac{\partial\Psi}{\partial t} = [H_0 + V(t)]\Psi \quad (\text{A1})$$

can be presented as the sum

$$\Psi(t) = \psi_0(t) + \sum_{\lambda} a_{\lambda}(t)\psi_{\lambda}(t) \quad (\text{A2})$$

over the set of eigenstates $\psi_{\lambda}(t)$ of the total Hamiltonian

$$i\frac{\partial\psi_{\lambda}}{\partial t} = [H_0 + V(t)]\psi_{\lambda},$$

which represent the possible final states of the system, $a_{\lambda}(t)$ being the amplitude of finding the system in one of these states. In Eq. (A2) we assume that $a_{\lambda}(t) \rightarrow 0$ at $t \rightarrow -\infty$ and the rate of the transition $\psi_0 \rightarrow \psi_{\lambda}$ is given by $d|a_{\lambda}(t)|^2/dt$.

According to the Floquet theorem, each state $\psi_{\lambda}(t) = e^{-iE_{\lambda}t}\phi_{\lambda}(t)$ is characterized by its quasienergy E_{λ} and the corresponding periodic quasienergy wave function $\phi_{\lambda}(t) = \phi_{\lambda}(t+T)$, found from

$$i\frac{\partial\phi_{\lambda}}{\partial t} = [H_0 + V(t) - E_{\lambda}]\phi_{\lambda}.$$

At any given t the quasienergy wave functions form a complete orthonormal set, $\langle\psi_{\lambda}|\psi_{\lambda'}\rangle = \langle\phi_{\lambda}|\phi_{\lambda'}\rangle = \delta_{\lambda\lambda'}$.

After inserting $\Psi(t)$ (A2) into Eq. (A1) and projecting it onto the state $\langle\psi_{\lambda}(t)|$, we arrive at

$$\begin{aligned} \frac{da_{\lambda}}{dt} &= -i\langle\psi_{\lambda}(t)|V(t)|\psi_0(t)\rangle \\ &= -ie^{iE_{\lambda}t}e^{-iE_0t}\langle\phi_{\lambda}(t)|V(t)|\phi_0\rangle. \end{aligned} \quad (\text{A3})$$

The last matrix element is a periodic function of time

$$\langle\phi_{\lambda}(t)|V(t)|\phi_0\rangle = \sum_n e^{-i\omega nt}A_{\lambda n}, \quad (\text{A4})$$

where $\omega = 2\pi/T$ and

$$A_{\lambda n} = \frac{1}{T} \int_0^T \langle\phi_{\lambda}(t)|V(t)|\phi_0\rangle e^{i\omega nt} dt. \quad (\text{A5})$$

Using (A4), we rewrite (A3) as

$$\frac{da_{\lambda}}{dt} = -i \sum_n e^{i(E_{\lambda} - E_0 - n\omega)t} A_{\lambda n}$$

and find

$$a_{\lambda} = \int^t \frac{da_{\lambda}}{dt} = - \sum_n \frac{e^{i(E_{\lambda} - E_0 - n\omega)t} e^{\eta t}}{E_{\lambda} - E_0 - n\omega - i\eta} A_{\lambda n},$$

where the energies E_{λ} have been given an infinitesimal shift $-i\eta$ to make $\int^t \dots dt$ converge at $-\infty$. The probability is given by

$$|a_{\lambda}|^2 = \sum_n \frac{e^{2\eta t} |A_{\lambda n}|^2}{(E_{\lambda} - E_0 - n\omega)^2 + \eta^2} + \text{oscillating terms}$$

and the rate is

$$\frac{d}{dt}|a_\lambda(t)|^2 = \sum_n \frac{2\eta e^{2n\eta}}{(E_\lambda - E_0 - n\omega)^2 + \eta^2} |A_{\lambda n}|^2,$$

where we dropped the oscillating terms since they do not contribute to the transition rate after we average it over a period. Finally, we take the limit $\eta \rightarrow 0$ using the following representation of the δ function:

$$\lim_{\eta \rightarrow 0} \frac{2\eta}{x^2 + \eta^2} = 2\pi \delta(x)$$

and obtain

$$\frac{d}{dt}|a_\lambda(t)|^2 = 2\pi \sum_n |A_{\lambda n}|^2 \delta(E_\lambda - E_0 - n\omega), \quad (\text{A6})$$

where the amplitude $A_{\lambda n}$ given by Eq. (A5) can be written as

$$A_{\lambda n} = \frac{1}{T} \int_0^T \langle \psi_\lambda(t) | V(t) | \psi_0(t) \rangle dt, \quad (\text{A7})$$

due to the energy conservation $E_\lambda - E_0 = n\omega$ implied by the δ function. This amplitude describes the n -quantum process and the total transition rate (A6) is the sum over all such processes. If the spectrum of λ is continuous, the differential transition rate dw_λ is proportional to the corresponding density of states $d\rho_\lambda$:

$$dw_\lambda = 2\pi \sum_n |A_{\lambda n}|^2 \delta(E_\lambda - E_0 - n\omega) d\rho_\lambda. \quad (\text{A8})$$

APPENDIX B: SADDLE-POINT METHOD FOR INTEGRALS WITH A SINGULARITY

Consider the integral

$$J = \int_C g(x) \exp[-\lambda f(x)] dx \quad (\text{B1})$$

for $\lambda \rightarrow \infty$. In this case it is well known [36] that the integration contour C should be deformed to go through the saddle point x_0 , where $f'(x_0) = 0$. The vicinity of this point gives the main contribution to the integral. If the function $g(x)$ is not singular at $x = x_0$, the integral (B1) is evaluated as

$$J \simeq g(x_0) \left(\frac{2\pi}{\lambda f''(x_0)} \right)^{1/2} \exp[-\lambda f(x_0)]. \quad (\text{B2})$$

If $g(x)$ has a singularity at $x = x_0$, e.g., $g(x) = (x - x_0)^{-\nu}$, the saddle-point answer has to be modified. Consider the following integral:

$$J_\nu = \int \frac{\exp[-\lambda f(x)]}{(x - x_0)^\nu} dx. \quad (\text{B3})$$

By using the transformation [27]

$$\frac{1}{(x - x_0)^\nu} = \frac{1}{\Gamma(\nu)} \int_0^\infty d\xi \xi^{\nu-1} \exp[-\xi(x - x_0)], \quad (\text{B4})$$

we turn (B3) into the double integral

$$\int_0^\infty d\xi \xi^{\nu-1} \int \exp[-\lambda f(x) - \xi(x - x_0)] dx. \quad (\text{B5})$$

Calculating $\int \dots dx$ by means of (B2) and then integrating over ξ , we obtain for $\lambda \rightarrow \infty$

$$J_\nu \simeq i^\nu \frac{\Gamma(\nu/2)}{2\Gamma(\nu)} \left(\frac{2\pi}{\lambda f''(x_0)} \right)^{1/2} [2\lambda f''(x_0)]^{\nu/2} \exp[-\lambda f(x_0)]. \quad (\text{B6})$$

For $\nu \rightarrow 0$ we, of course, recover (B2).

-
- [1] A. M. Dykhne, Zh. Éksp. Teor. Fiz. **38**, 570 (1960) [Sov. Phys. JETP **11**, 411 (1960)].
- [2] L. D. Landau and E. M. Lifshitz, *Quantum Mechanics. Non-relativistic Theory* (Pergamon, Oxford, 1965).
- [3] L. V. Keldysh, Zh. Éksp. Teor. Fiz. **47**, 1945 (1964) [Sov. Phys. JETP **20**, 1307 (1965)].
- [4] D. M. Volkov, Z. Phys. **94**, 250 (1935).
- [5] A. M. Perelomov, V. S. Popov, and M. V. Terent'ev, Zh. Éksp. Teor. Fiz. **50**, 1393 (1966) [Sov. Phys. JETP **23**, 924 (1966)]. Note that Eq. (53) of this paper contains a misprint in the phase factor before $\cos(\dots)$. The correct factor is $(-1)^{n+l+m}$ [see Eq. (42) of the present work].
- [6] F. H. M. Faisal, J. Phys. B **6**, L89 (1973).
- [7] H. R. Reiss, Phys. Rev. A **22**, 1786 (1980).
- [8] I. I. Fabrikant, Zh. Éksp. Teor. Fiz. **79**, 2070 (1980) [Sov. Phys. JETP **52**, 1045 (1980)].
- [9] Yu. N. Demkov, V. D. Kondratovich, and V. N. Ostrovsky, Pis'ma Zh. Éksp. Teor. Fiz. **34**, 425 (1981) [JETP Lett. **34**, 403 (1981)].
- [10] C. R. Liu, B. Gao, and A. Starace, Phys. Rev. A **46**, 5985 (1992).
- [11] M. Crance, J. Phys. B **21**, 3559 (1988).
- [12] C. Laughlin and S. I. Chu, Phys. Rev. A **48**, 4654 (1993).
- [13] H. W. van der Hart, Phys. Rev. A **50**, 2508 (1994).
- [14] D. Proulx, M. Pont, and R. Shakeshaft, Phys. Rev. A **49**, 1208 (1994).
- [15] L. Dimou and F. H. M. Faisal, J. Phys. B **27**, L333 (1994).
- [16] J. Wang, S. I. Chu, and C. Laughlin, Phys. Rev. A **50**, 3208 (1994).
- [17] D. A. Telnov and S. I. Chu, Phys. Rev. A **50**, 4099 (1994).
- [18] M. Dörr, J. Purvis, M. Terao-Dunseath, P. G. Burke, C. J. Joachain, and C. J. Noble, J. Phys. B **28**, 4481 (1995).
- [19] H. W. van der Hart, J. Phys. B **29**, 3059 (1996).
- [20] M. Yu. Kuchiev, Pis'ma Zh. Éksp. Teor. Fiz. **45**, 319 (1987) [JETP Lett. **45**, 404 (1987)].
- [21] M. Yu. Kuchiev, J. Phys. B **28**, 5093 (1995).
- [22] M. Yu. Kuchiev, Phys. Lett. A **212**, 77 (1996).

- [23] A. M. Perelomov and V. S. Popov, *Zh. Éksp. Teor. Fiz.* **52**, 514 (1967) [*Sov. Phys. JETP* **25**, 336 (1967)].
- [24] S. V. Fomichev and D. F. Zaretsky, *Phys. Lett. A* **144**, 91 (1990).
- [25] Yu. N. Demkov and G. F. Drukarev, *Zh. Éksp. Teor. Fiz.* **47**, 918 (1964) [*Sov. Phys. JETP* **20**, 614 (1965)].
- [26] B. M. Smirnov and M. I. Chibisov, *Zh. Éksp. Teor. Fiz.* **49**, 841 (1965) [*Sov. Phys. JETP* **22**, 585 (1966)]. The incorrect numerical coefficient in Eq. (11) of this paper was corrected in [5].
- [27] I. S. Gradshtein and I. M. Ryzhik, *Tables of Integrals, Series, and Products* (Academic Press, Boston, 1994).
- [28] D. A. Varshalovich, A. N. Moskalev and V. K. Khersonskii, *Quantum Theory of Angular Momentum: Irreducible Tensors, Spherical Harmonics, Vector Coupling Coefficients, 3nj symbols* (World Scientific, Singapore, 1988).
- [29] Note that the final answer for the probability presented in [3] [Eq. (16)] is two times smaller than one would get from (25), neglecting the interference between the two terms. This could possibly mean that the contribution of only one saddle point has been taken into account in [3].
- [30] I. I. Fabrikant, *J. Phys. B* **26**, 2533 (1993).
- [31] S. Wolfram, *Mathematica: A System for Doing Mathematics by Computer*, 2nd ed. (Addison-Wesley Publishing Co., Palo Alto, 1991).
- [32] E. E. Nikitin and B. M. Smirnov, *Atomic and Molecular Processes* (Nauka, Moscow, 1988).
- [33] H. Hotop and W. C. Lineberger, *J. Phys. Chem. Ref. Data* **14**, 731 (1985).
- [34] A. A. Radtsig and B. M. Smirnov, *Parameters of Atoms and Atomic Ions: Handbook* (Energoatomizdat, Moscow, 1986).
- [35] M. Crance, *J. Phys. B* **20**, L411 (1987); *ibid.* **20**, 6553 (1987).
- [36] E. T. Copson, *Asymptotic Expansions* (Cambridge University Press, Cambridge, England, 1965).